Surrogate-Driven Multi-Objective Predictive Control for Electric Vehicular Platoon

Wu, Yanhong; Zuo, Zhiqiang; Wang, Yijing; Han, Qiaoni; Li, Ji; Zhou, Quan; Xu, Hongming

DOI:
10.1109/TTE.2024.3379590

Surrogate-Driven Multi-Objective Predictive Control for Electric Vehicular Platoon

Yanhong Wu, Zhiqiang Zuo, *Senior Member, IEEE*, Yijing Wang, Qiaoni Han, Ji Li, *Member, IEEE*, Quan Zhou, *Member, IEEE*, Hongming Xu

***Abstract*—This paper proposes a surrogate-driven multi-objective predictive control (SMPC) strategy to address the dynamics uncertainty and multi-objective optimization issues of electric vehicular platoon (EVP). A surrogate-driven model is established with subspace identification to alleviate the adverse effects of uncertain dynamics for EVP. Then, a subspace predictor-based distributed surrogate-driven model predictive controller is developed for EVP. To mitigate conflicts among multiple optimization objectives involving driving safety, driving comfort and energy economy, a multi-objective cost function with the predictive sequence is designed. To this end, a grey wolf optimizer is suggested to guide the search towards diverse solutions, aiming to achieve globally optimal trade-offs among conflicting multiple objectives. In this way, the SMPC strategy is constructed, and its stability is theoretically proven. Finally, several experiments are carried out on a co-simulation vehicular platoon platform with the IPG-CarMaker software. The experimental results validate the effectiveness of the proposed SMPC strategy.**

***Index Terms*—Electric vehicular platoon, multi-objective optimization, surrogate-driven model predictive control, grey wolf optimization.**

I. Introduction

The burgeoning requirement for intelligent transportation system has encountered obstacles due to limited road capacity, increasing concerns about traffic safety and the intensifying energy crisis. The promotion of autonomous electric vehicle (AEV) constitutes a long-time strategic goal by the transportation community [1]. Therefore, it is essential to design a suitable strategy to strike a balance among driving safety, driving comfort and energy economy for electric vehicular platoon (EVP).

Powertrain modelling constitutes a pivotal element in the optimization of AEV performance. Actually, each AEV has a complex structure involving motor, battery, transmission and chassis. As a result, it is hard to dissect the accurate physical parameters [2]. To this end, extensive research has been conducted to alleviate the adverse effects of uncertain dynamics, thereby ensuring the inter-spacing of EVP [3]–[6]. However, focusing solely on the safety of EVP while disregarding their economic viability and comfort implications poses significant risks [7], [8]. In detail, disregarding economic dimension may generate heavy financial burden, thus impeding their widespread acceptance [9]. Concurrently, disregarding comfort facets could potentially evoke user discontent and engender resistance towards the assimilation of novel technologies. Therefore, a suitable solution is expected to integrate the safety, economy and comfort of EVP. As a result, the exploitation of multi-objective optimization approach has triggered a widespread research upsurge.

Among plenty of existing platoon control schemes, the distributed model predictive control has attracted considerable attention [10], [11]. For the distributed model predictive control scheme, each controller solves individual optimal control problem within a finite horizon and exchanges information over the communication network [12]. This approach relies on an accurate dynamic model and becomes impractical for several intricate dynamic systems, especially for AEV [13]–[15]. In light of this predicament, the surrogate-driven modelling method provides a feasible solution with rapid evolution in data collection, storage and processing capabilities. The underlying principle of this focuses on examining the real-time input-output (I/O) trajectory to identify the black-box system [16]. One of the representatives is Network-based model predictive control, namely, surrogate-driven model predictive control [17], [18]. It should be pointed out that this scheme would cause a substantial computational burden. Then, a subspace-based surrogate-driven modelling approach has emerged with satisfactory computational efficiency [19]. Its subspace linear predictor can be directly employed in the predictive process without identifying the local state-space model. Therefore, these studies inspire us to develop an efficient surrogate-driven predictive control strategy for EVP.

In practice, keeping the inter-spacing of EVP does not imply that the optional performance can be achieved. The energy economy and driving comfort also are important indicators [20], [21]. These indicators directly influence the driving experience and the acceptance of autonomous driving technology in the transportation ecosystem. The essence of this task pertains to a multi-objective optimization problem. Therefore, a hierarchical multi-objective optimization scheme considering fuel consumption minimization and traffic safety improvement was developed in [22]. To simplify the multi-objective problem, the Pareto method and weighted-sum method provide feasible ideas, and then multiple objectives can be integrated into

This work was supported by the National Natural Science Foundation of China under Grant 62173243, Grant 61933014 and Grant 61803218, in part by the Open Research Program of the Key Laboratory of System Control and Information Processing, Ministry of Education, under Grant Scip202101. (Correspoonding Authors: Qiaoni Han and Ji Li).

Yanhong Wu, Zhiqiang Zuo, Yijing Wang and Qiaoni Han are with the Tianjin Key Laboratory of Intelligent Unmanned Swarm Technology and System, School of Electrical and Information Engineering, Tianjin University, Tianjin, 300072, China (e-mails: yanhongwu@tju.edu.cn; zqzuo@tju.edu.cn; yjwang@tju.edu.cn; qnhan@tju.edu.cn.)

Ji Li, Quan Zhou and Hongming Xu are with the Department of Mechanical Engineering, University of Birmingham, Birmingham B15 2TT, U.K. (e-mails: J.Li.1@bham.ac.uk; q.zhou@bham.ac.uk; h.m.xu@bham.ac.uk.)

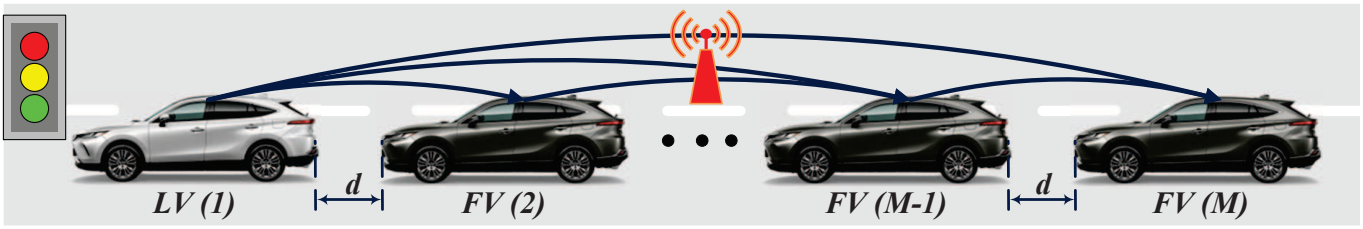

Fig. 1. Schematic diagram of vehicular platoon with PLF communication topology

one single objective [23]. In this way, several optimization approaches such as particle swarm optimization [24], genetic optimization [25], ant colony optimization [26] and grey wolf optimization (GWO) [27] have been put forward. Among them, GWO adeptly maintains a diversified pool along the Pareto front, thereby enhancing its capacity to capture a comprehensive spectrum of trade-off solutions. It is noted that GWO may occasionally get stuck in local optimal, failing to find the global optimum. To enhance global exploration capability, an annealing-based GWO was developed in [28]. Nevertheless, these multi-objectives optimization schemes only rely on current conditions, and they may fall short in addressing intricate and dynamically evolving traffic scenarios.

The aforementioned research in vehicular platoon modelling is dedicated to constructing dynamic models rather than surrogate-driven ones. This brings a challenge in obtaining accurate dynamic parameters for EVP. Furthermore, the existing control algorithms are hard to balance multi-objectives conflicts in complex driving scenarios. All these factors motivate us to develop an accurate platoon model and an efficient multi-objective optimization scheme for EVP. The main contributions of this paper are summarized below.

i) A subspace-based surrogate-driven modelling method is developed to characterize the EVP dynamics. The electric vehicular model includes driving motor, battery, transmission and chassis, and it is arduous to obtain these complex dynamic parameters. Therefore, the subspace technology is employed to construct a surrogate-driven model. This model can be directly utilized to the prediction process without identifying the local state-space model, thereby enhancing the applicability of EVP model.

ii) A surrogate-driven multi-objective predictive control (SMPC) strategy is proposed to solve the multi-objective issue involving driving safety, driving comfort and energy economy. It combines the predictive capabilities of model predictive controller with the global optimization performance of GWO. Such a treatment could optimally balance the multi-objective conflicts and reduce the computational burden.

iii) An EVP co-simulation platform is established with the Matlab software and the IPG-CarMaker software. Several field experiments are conducted to verify the effectiveness of our proposed strategy.

This paper is organized as follows. Section II illustrates the vehicular platoon model. Section III designs the SMPC strategy. Field experiments are carried out in Section IV. Experimental results are analyzed in Section V. Section VI draws the conclusion.

Notations: $\|\cdot\|_{\mathrm{II}}$ stands for the Frobenius norm. The Moore-Penrose pseudo inverse of matrix H is denoted as $H^{\dagger}$. $|A|$ denotes the absolute of A. $\|\cdot\|^2$ represents the L_2 norm.

II. Vehicle Modelling

The EVP consists of one leading vehicle (LV) and $M-1$ following vehicles (FV). The predecessor-leader following (PLF) communication topology is utilized to characterize the relationship between the preceding vehicle and the following ones [4]. Each AEV involves motor, battery, transmission and chassis. To alleviate the adverse effects of uncertain dynamics, the mechanism model is transformed into a surrogate-driven one.

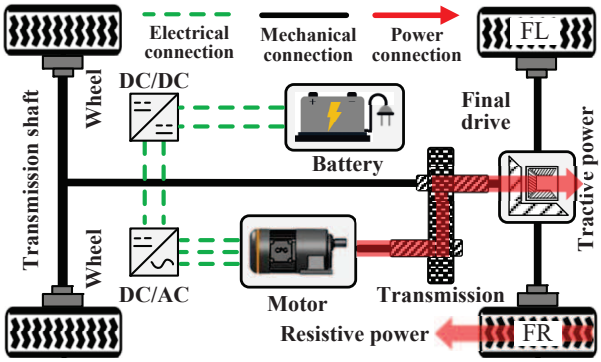

Fig. 2. Schematic diagram of AEV

A. Mechanism Model

Fig. 2 gives the powertrain structure of AEV. The battery could generate direct current which is converted to alternating current to steer the motor. Wheels are propelled by the motor through the transmission, and they also suffer the resistance [29]. To derive a concise model, several reasonable hypotheses are given: 1) The vehicle is traveling on a dry and flat road, with negligible longitudinal slip of the tires. 2) The vehicle body is symmetric and rigid. 3) The yaw and pitch motions of the vehicle are neglected. 4) The influences of internal resistance, temperature variation and capacity degradation on the battery are ignored [30], [31].

The actual driving torque of AEV is expressed as

$$T_t = T_e i_g \eta_t$$

where T_t denotes the driving torque from the transmission. T_e represents the demand torque. i_g is the transmission ratio. η_t stands for the transmission efficiency.

The vehicle kinematics model is provided to describe the characteristics of AEV. Specifically,

$$\begin{cases} T_t = FR \\ F = ma \\ \dot{S} = V \\ \dot{V} = a \end{cases}$$

where F denotes the driving force. R represents the tire radius. m stands for the vehicle mass. S is the position. V represents the velocity. a denotes the acceleration.

The current I is generated through the motor [32], and it has the form

$$I = \frac{T_e N_t}{95U} \approx \frac{T_e}{K_e} \tag{1}$$

where K_e denotes the anti-electromotive force coefficient. N_t and U are the speed and voltage of the motor.

The state of charge (SOC) of the battery is described as

$$\mathrm{SOC} = \mathrm{SOC}_0 - \int \frac{I}{C_{bat}} dt$$

where SOC_0 denotes the initial condition of SOC. C_{bat} stands for the capacity of the battery.

With the above formulas, we can get

$$\begin{cases} \dot{S} = V \\ \dot{V} = \dfrac{T_e i_g \eta_t}{mR} \\ \dot{\mathrm{SOC}} = -\dfrac{T_e}{K_e C_{bat}} \end{cases}$$

According to the properties of PLF communication topology in Fig. 1, FV i could receive the information of LV 1. LV 1 has the optimal velocity, spacing and SOC, which are regarded as the reference states. Then, the Taylor formula is introduced to build an error model of the i^{th} AEV. That is

$$\mathcal{X}_i(k+1) = \mathcal{A}_i(k)\mathcal{X}_i(k) + \mathcal{B}_i(k)\mathcal{U}_i(k) \tag{2}$$

with

$$\mathcal{A}_i(k) = \begin{bmatrix} 1 & 0 & 0 \\ 0 & T_s + 1 & 0 \\ 0 & 0 & 1 \end{bmatrix}, \mathcal{B}_i(k) = \begin{bmatrix} T_{e,i} i_{g,i} \eta_{t,i} T_s/(m_i R_i) \\ 0 \\ -T_s/(K_{e,i}\ C_{bat,i}) \end{bmatrix},$$

$$\mathcal{X}_i(k) = \begin{bmatrix} \widetilde{V}_i(k) \\ \widetilde{S}_i(k) \\ \widetilde{\mathrm{SOC}}_i(k) \end{bmatrix} = \begin{bmatrix} V_i(k) - V_1(k) \\ S_i(k) - S_1(k) - di \\ \mathrm{SOC}_i(k) - \mathrm{SOC}_1(k) \end{bmatrix},$$

$$\mathcal{U}_i(k) = \begin{bmatrix} \widetilde{T}_{e,i}(k) \end{bmatrix} = \begin{bmatrix} T_{e,i}(k) - T_{e,1}(k) \end{bmatrix},$$

where T_s stands for the sampling period. d represents the spacing. Subscript 1 denotes the leading vehicle. Note that

Among the existing complex characteristics, there are several uncertain parameters such as m, R, K_e and C_{bat}. To address this issue, a surrogate-driven model approach will be developed in the following subsection.

B. Surrogate-driven Model

The subspace identification method has its proficiency in surrogate-driven modelling by identifying underlying low-dimensional structures in high-dimensional data. This approach facilitates accurate representation, analysis, and prediction of complex vehicle dynamics. To certain extent, it could enhance model interpretability and reduce computational complexity [33]. Therefore, we employ it to construct the surrogate-driven model for EVP.

The control output $\mathcal{Y}_i(k)$ is made up of state vector with $\mathcal{Y}_i(k) = C\mathcal{X}_i(k)$. Here, C_i is an identity matrix. Then, the I/O trajectory for prediction horizon N and excitive order L is stacked up to construct Hankel matrices. That is,

$$\mathcal{Y}_i^f(k) = \Gamma_i(k)\mathcal{X}_i^f(k) + \mathcal{H}_i(k)\mathcal{U}_i^f(k) \tag{3a}$$

$$\mathcal{Y}_i^p(k) = \Gamma_i(k)\mathcal{X}_i^p(k) + \mathcal{H}_i(k)\mathcal{U}_i^p(k) \tag{3b}$$

with

$$\mathcal{Y}_i^p(k) = \begin{bmatrix} \mathcal{Y}_i(k) & \cdots & \mathcal{Y}_i(k+N-L) \\ \vdots & \ddots & \vdots \\ \mathcal{Y}_i(k+L-1) & \cdots & \mathcal{Y}_i(k+N-1) \end{bmatrix},$$

$$\mathcal{Y}_i^f(k) = \begin{bmatrix} \mathcal{Y}_i(k+L) & \cdots & \mathcal{Y}_i(k+N) \\ \vdots & \ddots & \vdots \\ \mathcal{Y}_i(k+2L-1) & \cdots & \mathcal{Y}_i(k+L+N-1) \end{bmatrix},$$

$$\mathcal{X}_i^p(k) = \begin{bmatrix} \mathcal{X}_i(k) & \cdots & \mathcal{X}_i(k+N-L) \end{bmatrix},$$

$$\mathcal{X}_i^f(k) = \begin{bmatrix} \mathcal{X}_i(k+L) & \cdots & \mathcal{X}_i(k+N) \end{bmatrix},$$

$$\Gamma_i(k) = \begin{bmatrix} C_i(k) & C_i(k)\mathcal{A}_i(k) & \cdots & C_i(k)\mathcal{A}_i^{L-1}(k) \end{bmatrix}^T,$$

$$\mathcal{H}_i(k) = \begin{bmatrix} 0 & C_i(k)\mathcal{B}_i(k) & \cdots & C_i(k)\mathcal{A}_i^{L-2}(k)\mathcal{B}_i(k) \\ 0 & 0 & \cdots & C_i(k)\mathcal{A}_i^{L-3}(k)\mathcal{B}_i(k) \\ \vdots & \vdots & \ddots & \vdots \\ 0 & 0 & \cdots & 0 \end{bmatrix}^T,$$

$\mathcal{U}_i^f(k)$ and $\mathcal{U}_i^p(k)$ have similar forms as $\mathcal{Y}_i^f(k)$ and $\mathcal{Y}_i^p(k)$, where superscripts p and f denote the past and future matrices of the variables.

So far, the mechanism model (2) has been converted to a surrogate-driven one (3), and it will be employed to design the control strategy.

III. SMPC Strategy Design

In this section, the SMPC strategy is suggested by combining the GWO-based multi-objective optimization method and the distributed surrogate-driven model predictive control approach. Furthermore, the stability of EVP is analyzed. Fig. 3 depicts the framework of the SMPC strategy. More specifically, the surrogate-driven EVP model is implemented to construct the subspace predictor of the model predictive control, and it could generate the predictive sequence. Based on this, a multi-objective cost function involving driving safety, driving comfort and economy is calculated by GWO. Then, the optimal control sequence is obtained to steer EVP.

A. Subspace Predictor

The Hankel matrices in (3) are derived as the subspace-based linear predictor. The rationale behind adopting a subspace predictor lies in employing data mapping techniques to formulate a novel surrogate-driven model, thereby efficiently mitigating control issues caused by modelling errors. These approach can be directly employed in the prediction process without identifying the local state-space model [34].

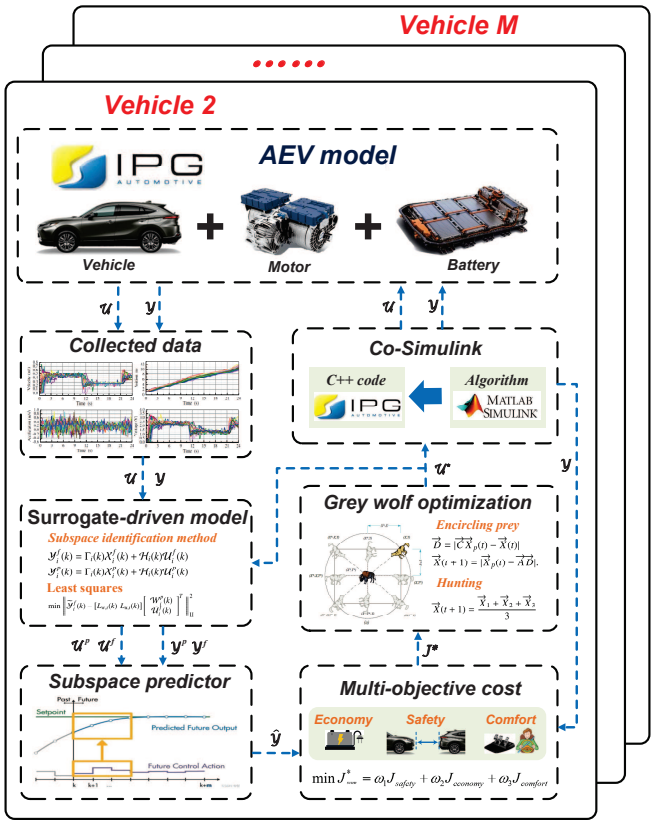

Fig. 3. The framework of the SMPC strategy

By introducing the least squares scheme to calculate $L_{w,i}(k)$ and $L_{u,i}(k)$, the optimization problem can be formulated as

$$\min \left\| \mathcal{Y}_i^f(k) - [L_{w,i}(k)\ L_{u,i}(k)] \begin{bmatrix} \mathcal{W}_i^p(k) \\ \mathcal{U}_i^f(k) \end{bmatrix} \right\|_{\Pi}^2 \tag{4}$$

where $\mathcal{W}_i^p(k) = [\mathcal{Y}_i^p(k)\ \mathcal{U}_i^p(k)]^T$ stands for the subspace prediction matrix corresponding to the past I/O trajectory. $L_{u,i}(k)$ and $L_{w,i}(k)$ denote the subspace linear predictor coefficients.

Then, the orthogonal projection technique is suggested to calculate the least squares problem in (4). Thus,

$$\hat{\mathcal{Y}}_i(k) = \mathcal{Y}_i^f(k) \Big/ \left[\mathcal{W}_i^p(k)\ \mathcal{U}_i^f(k)\right]^T.$$

According to the properties of QR-decomposition, we can obtain

$$\begin{aligned} \hat{\mathcal{Y}}_i(k) &= \mathcal{Y}_i^f(k) \begin{bmatrix} \mathcal{W}_i^p(k) \\ \mathcal{U}_i^f(k) \end{bmatrix}^{\dagger} \begin{bmatrix} \mathcal{W}_i^p(k) \\ \mathcal{U}_i^f(k) \end{bmatrix} \\ &= \begin{bmatrix} L_{w,i}(k)\ L_{u,i}(k) \end{bmatrix} \begin{bmatrix} \mathcal{W}_i^p(k) \\ \mathcal{U}_i^f(k) \end{bmatrix}. \end{aligned} \tag{5}$$

Furthermore, the model predictive control algorithm offers a significant benefit in handling operational constraints of the cost function [30]. That is

$$\begin{aligned} \mathcal{Y}_i^{min} \le \mathcal{Y}_i(k+\tau|k) \le \mathcal{Y}_i^{max} \\ \mathcal{U}_i^{min} \le \mathcal{U}_i(k+\tau|k) \le \mathcal{U}_i^{max} \end{aligned}$$

where superscripts *min* and *max* denote the lower and upper bounds of the constraints.

The predicted output sequence $\hat{\mathcal{Y}}_i(k)$ will be used to design the following multi-objective cost function.

B. Multi-Objective Cost Function

The multi-objective optimization of EVP has received significant attention [35]. It is pivotal in ensuring an efficient driving experience, aligning with both driving safety and economic consideration [23]. Here, a multi-objective cost function with predictive sequences is constructed in the sequel.

Three optimization objectives involving driving safety, driving comfort and energy economy correspond to distinct predictive variables ($\hat{\mathcal{Y}}$). The velocity and control torque are crucial indicators for ensuring driving comfort, while spacing and SOC are determinants of driving safety and energy economy. Note that the predictive sequences of the preceding vehicle $i-1$ are regarded as the optimal objectives for ego vehicle i. The economic objective aims to maintain a consistently high SOC, closing to SOC of reference states. In this way, three cost functions concerning safety, comfort and economy are respectively defined as

$$J_i^s(k) = min \sum_{\tau=0}^{N-1} \| \widetilde{S}_i(k+\tau|k) - \widetilde{S}_{i-1}(k+\tau|k) - d \|^2 \tag{6}$$

$$\begin{aligned} J_i^c(k) = min \sum_{\tau=0}^{N-1} \Big(& \| \widetilde{V}_i(k+\tau|k) - \widetilde{V}_{i-1}(k+\tau|k) \|_{Q_i}^2 \\ & + \| \widetilde{T}_{e,i}(k+\tau|k) \|_{R_i}^2 \Big) \end{aligned} \tag{7}$$

$$J_i^e(k) = min \sum_{\tau=0}^{N-1} \| \widetilde{\mathrm{SOC}}_i(k+\tau|k) \|^2 \tag{8}$$

where Q and R are the weight coefficients of velocity and input torque.

Each objective has been well addressed in [36], [37]. More specific,

1) Driving safety J_i^s: Driving safety refers to the ability to prevent accidents and minimize potential risks within the traffic system. The objective of driving safety aims to improve the position tracking performance by adjusting the inter-vehicle spacing. Here, it requires a desired platoon spacing between ego vehicle i and the preceding vehicle $i-1$.
2) Driving comfort J_i^c: Driving comfort seeks to meet the user's driving experience. The purpose of this item is to provide smooth and moderate speed variations, minimizing discomfort and bumps during acceleration and braking processes. Specially, it should minimize velocity error for ego vehicle i and preceding vehicle $i-1$. In addition, the control input $\widetilde{T}_e$ should also stay within a reasonable range.
3) Energy economy J_i^e: Energy economy is vital for improving driving range and enhancing economic efficiency. This object represents the ability to minimize battery consumption with the goal of achieving efficient energy utilization. Each vehicle is required to ensure a stable discharge process by reducing SOC deviation from the optimal value.

The process of solving multi-objective optimization is fraught with inherent challenges. One of the pivotal difficulties comes from the intricate task of simultaneously optimizing multiple conflicting objectives. Therefore, the weighted-sum scheme integrates different objectives into one single objective with configurable weights. This efficient approach demonstrates remarkable performance in addressing complex multi-objective issue, particularly in practical applications where computational resources are limited [35].

From (6)-(8), the sum cost function can be represented by

$$J_i^*(k) = min \sum_{\varsigma=1}^{3} w_\varsigma J_i^\varsigma(k) = min \sum_{\tau=0}^{N-1} \xi\Big(\mathcal{Y}_i(k+\tau|k), \mathcal{U}_i(k+\tau|k)\Big)$$
$$s.t. \quad w_\varsigma > 0, \ \sum_{\varsigma=1}^{3} w_\varsigma = 1, \ \varsigma = \{s, c, e\} \tag{9}$$

where w_ς denotes the weight coefficients corresponding to each objective. Previous studies [23], [38] have given the recommended values of $w_\varsigma = [0.5, 0.25, 0.25]$.

Then, each sum cost function J_i^* with prediction sequence is subject to optimization in terms of the following GWO algorithm.

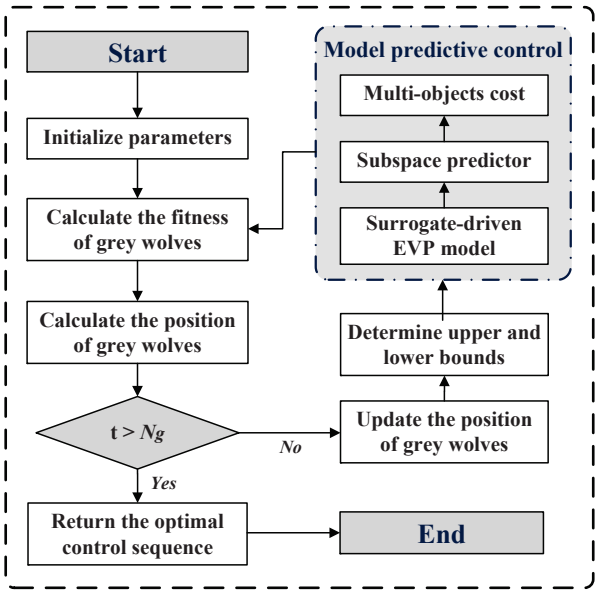

Fig. 4. The flowchart of the SMPC strategy

C. Grey Wolf Optimization

Actually, the GWO algorithm has emerged as a nature-inspired metaheuristic algorithm that demonstrates distinctive efficacy in addressing the global optimization issue [39]. GWO could maintain diversity within the solution space by emulating the collaborative and individualistic tendencies of grey wolves. The wolves with the best fitness values are regarded as leading wolves (α, β and δ). The grey wolf, denoted as ω, represents the residual individuals within the wolf pack. Under the leadership of wolves α, β and δ, a continuous search for the optimal solution in multi-objective optimization is conducted.

In the encircling prey step, the grey wolves surround the prey during the hunt. This behavior is modeled as

$$\begin{cases} D(t) = |\mathscr{C} P_p(t) - P(t)|, \ t \in [1, N_g] \\ P(t+1) = P_p(t) - \mathscr{A} D(t) \end{cases} \tag{10}$$

with

$$\mathscr{A} = 2ar_1 - a, \ r_1 \in [0, 1]$$
$$\mathscr{C} = 2ar_2, \ r_2 \in [0, 1]$$

where P and P_p represent the population positions of the wolf ω and the prey at the t^{th} iteration step, respectively. N_g denotes the maximum number of iterations. D is the distance between the wolf ω and the prey. $\mathscr{A}$ and $\mathscr{C}$ represent the coefficient vectors, which are determined by the convergence factor a and random vectors (r_1, r_2). Such a treatment could mitigate local optimum stagnation and enhance the exploration speed by assigning random weights to the prey. Here, the optimal control input T_e is derived from the population position of grey wolf and is then implemented to drive AEVs.

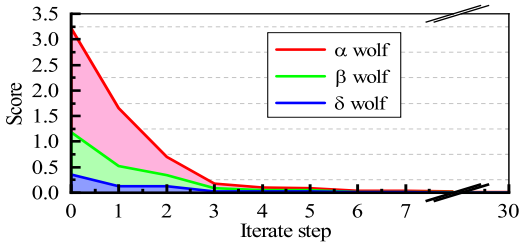

Fig. 5. The convergence performance of GWO

Fig. 4 plots the detailed solving process of GWO. Note that the fitness function is responsible for scalarizing the sum cost function into unified scores. These scores are assigned to different wolves α, β and δ for discerning the quality of each solution. As shown in Fig. 5, the scores of wolves α, β and δ could converge within 6 iterative steps. This indicates that the proposed strategy executes effective performance in addressing multi-objective optimization problems.

D. Stability Analysis

The stability is essential to ensure that the algorithm consistently converges to an optimal equilibrium while addressing complex optimization issues. Therefore, the detailed stability analysis of the proposed strategy is carried out in this subsection.

Lemma 1: [16] System (2) is characterized by the stabilizability and the detectability. If system (2) is stable, there exists a Lyapunov function $W_i(k)$ fulfills

$$W_i(k+1) - W_i(k) \le -\varepsilon_0 \|\mathcal{X}_i(k)\|^2 + \xi\Big(\mathcal{Y}_i(k), \mathcal{U}_i(k)\Big) \tag{11}$$
$$s.t. \quad W_i(k) \le \gamma_0 \|\mathcal{X}_i(k)\|^2, W_i^N(k) = \textstyle\sum_{\tau=0}^{N-1} W_i(k+\tau|k)$$

where ε_0 and γ_0 are positive constants.

By combining the quadratic stage cost with an exponential controllability argument, it guarantees the boundedness of infinite horizon cost, i.e.,

$$J_i^*(k) \le \gamma_s \|\mathcal{X}_i(k)\|^2, \ \gamma_s > 0. \tag{12}$$

Then, a local Lyapunov function candidate $V_i(k)$ is constructed as

$$V_i(k) = J_i^*(k) + W_i^N(k). \tag{13}$$

Theorem 1: Suppose that $\{\mathcal{U}_i^p, \mathcal{U}_i^f\}$ is persistently exciting of order $N + 2n$. For any constant $\Upsilon > 0$, there always exists a horizon $N_m > 0$ such that for all $N > N_m$ and any initial condition satisfying $V_i(0) < \Upsilon$, the SMPC problem (9) is recursively feasible. Then, the closed-loop system is stable if the function $V_i(k)$ satisfies $\varepsilon_0\|\mathcal{X}_i(k)\|^2 \le V_i(k) \le \gamma_s\|\mathcal{X}_i(k)\|^2$ and $\frac{\gamma_s(\gamma_s-\gamma_o)}{\varepsilon_0(N_m-1)} - \varepsilon_0 \le 0$.

Proof: With (11)-(13), the lower bound and upper bound of $V_i(k)$ can be obtained

$$\varepsilon_0\|\mathcal{X}_i(k)\|^2 \le V_i(k) \le \gamma_s\|\mathcal{X}_i(k)\|^2 + \gamma_0\|\mathcal{X}_i(k)\|^2. \tag{14}$$

According to *Lemma* 1, the detectability property (11) yields

$$\begin{aligned} &W_i^N(k+1) - W_i^N(k) \\ &= \sum_{\tau=0}^{N-1}\Big(W_i(k+\tau+1|k+1) - W_i(k+\tau|k)\Big) \\ &\le -\sum_{\tau=0}^{N-1}\Big(\varepsilon_0\|\mathcal{X}_i(k)\|^2\Big) + \sum_{\tau=0}^{N-1}\xi\Big(\mathcal{Y}_i(k+\tau|k), \mathcal{U}_i(k+\tau|k)\Big). \end{aligned} \tag{15}$$

From (14) and (15), we can get

$$\sum_{k=1}^{N-1}\Big(\varepsilon_0\|\mathcal{X}_i(k)\|^2\Big) \le V_i(k) \le (\gamma_s + \gamma_0)\|\mathcal{X}_i(k)\|^2.$$

Thus, there exists an integer $N_m \in \{1, 2..., N-1\}$ such that

$$\|\mathcal{X}_i(k)\|^2 \le \frac{\gamma_s + \gamma_0}{\varepsilon_0(N_m - 1)}\|\mathcal{X}_i(k)\|^2.$$

Denote the standard candidate solution being $\{\mathcal{Y}_i'(k+1|k), \mathcal{U}_i'(k+1|k)\}$, then one derives

$$\begin{aligned} J_i'(k+1) &= \sum_{\tau=0}^{N-1}\xi\Big(\mathcal{Y}_i'(k+\tau+1|k+1), \mathcal{U}_i'(k+\tau+1|k+1)\Big) \\ &= J_i^*(k) - \xi\Big(\mathcal{Y}_i^*(k|k), \mathcal{U}_i^*(k|k)\Big). \end{aligned}$$

Hence, it follows that

$$J_i^*(k+1) \le J_i^*(k) - \xi\Big(\mathcal{Y}_i^*(k|k), \mathcal{U}_i^*(k|k)\Big).$$

Then, the cost of the candidate solution over the horizon N_m satisfies

$$\begin{aligned} &J_i^*(k+1) + \xi(\mathcal{Y}_i(k|k), \mathcal{U}_i(k|k)) \\ &\le \sum_{\tau=0}^{N_m-1}\xi\Big(\mathcal{Y}_i^*(k+\tau|k), \mathcal{U}_i^*(k+\tau|k)\Big) + J_i^*(k+1) \\ &\le J_i^*(k) + \frac{\gamma_s + \gamma_0}{\varepsilon_0(N_m - 1)}\|\mathcal{X}_i(k)\|^2. \end{aligned} \tag{16}$$

According to (14) and (16), the Lyapunov function candidate admits

$$V_i(k+1) - V_i(k) \le \frac{\gamma_s + \gamma_0}{\varepsilon_0(N_m - 1)}\|\mathcal{X}_i(k)\|^2 - \varepsilon_0\|\mathcal{X}_i(k)\|_2^2.$$

To ensure $V_i(k)$ being decreased monotonically, a sufficiently long horizon N_m is required, that is

$$N \ge N_m \ge \frac{\gamma_s + \gamma_0}{\varepsilon_0^2} + 1.$$

Now it can be concluded that the SMPC scheme is stable, thus achieving vehicular platoon tracking. This completes the proof. ■

Here, the prediction horizon N is chosen as 16. Note that the control horizon is set to be consistent with the prediction horizon N. This consistency allows simultaneous consideration of prediction and control within the same scale, reducing the complexity of optimization problem [4].

In addition to prediction horizon N, sampling time T_s also plays a significant role in the performance of MPC [40]. The above two parameters determine the prediction time T_N of MPC, where $T_N = T_s * N$. To ensure the stability of platoon, T_N should satisfy [41]

$$T_N \ge \frac{V_{max}}{a_{max}} + \frac{2a_{max}^3}{3J_{max}^2}$$

where V_{max}, a_{max} and J_{max} represent maximum velocity, maximum acceleration and maximum jerk of the vehicle, respectively. With this in mind, T_s is chosen as $10Hz$.

IV. Experiments Design

In this section, a co-simulation experimental platform is designed with IPG-CarMaker® software. Then, several comparison experiments are conducted to verify the effectiveness of the proposed SMPC strategy.

A. Experimental Platform

The experiment is carried out on a vehicular platoon co-simulation platform (see Fig. 6) with Matlab® software and IPG-CarMaker® software and high-performance computer. This computer is equipped with an Intel i7-14700KF (3.4GHz) CPU and an RTX4060 GPU, which meets the computational requirements for the actual vehicle applications [42], [43]. IPG-CarMaker® details AEV dynamics including chassis, battery, motor, clutch, engine and tire models.

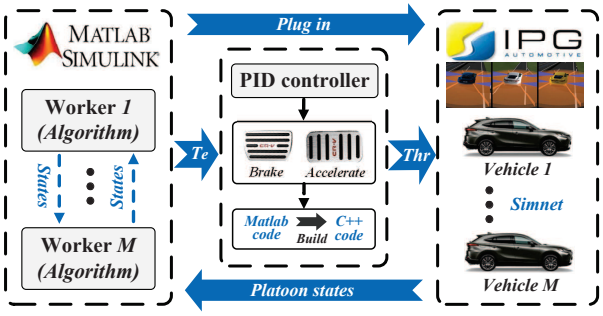

Fig. 6. Experimental framework of vehicular platoon platform

The proposed SMPC strategy is deployed with Matlab language on the host computer, and it could generate the optimal control sequence (T_e). However, it is not feasible

that T_e is directly used to drive AEV. Therefore, a PID-based lower-level controller is designed. In this way, each AEV is driven via brake and acceleration to track T_e, thus achieving platoon control. The algorithm is compiled into C++ code and plugged in the IPG-CarMaker® software. In addition, the real-time information of vehicular platoon could be exchanged through the SimNet module. The SimNet add-on for IPG-CarMaker® allows a connection of multiple vehicles running in an independent CarMaker application. This forms a closed-loop structure.

TABLE I: VEHICULAR PARAMETERS

Symbol	m (kg)	R (m)	i_g	C_{bat} (Ah)	K_e
L_1	1891	0.334	0.89	190	3.8
F_1	1401	0.317	0.85	105	3.2
F_2	2100	0.341	0.86	110	3.4

The EVP configuration with three AEVs traveling on a 9km straight road with ideal conditions. Such a platoon size could meet the requirements for platoon testing [44]. The default vehicle models of platoon including *CompanyCarEV* (leading vehicle 1, L_1), *MyBatteryCU* (following vehicle 2, F_2) and *Tesla modelS* (following vehicle 3, F_3) are chosen from IPG-CarMaker®. The reference velocity of L_1 follows a predefined drive cycle source block (FTP75) from Simulink. This block simulates various driving speeds encountered in urban traffic, which accommodates frequent idling, stopping and acceleration situations. As stated in Ref. [45], the general headway time (T_h) is 2-3s, which could ensure vehicles have sufficient response time to avoid collisions. The minimum safe spacing (S_{min}) should satisfies $S_{min} \geq T_h * V$. Here, the desired safe spacing is set to 50m. TABLE I lists the relevant vehicle dynamic parameters.

B. Experimental Procedure

The experimental procedure is divided into two stages: data collection stage and strategy verification stage. At the first stage, all AEVs are driven by the default control module of IPG-CarMaker®. The collected vehicular platoon dataset is utilized to train the surrogate-driven model. For the second stage, L_1 is regarded as a leading vehicle while different control strategies are embedded into the following vehicles (F_2, F_3).

TABLE II: DIFFERENCES OF EXPERIMENTS

Merits	***Exp1***	***Exp2***	***Exp3***
Modelling	Mechanism	Surrogate	Surrogate
Solver	LQR	LQR	GWO

Three different experiments are conducted to validate the performance of our proposed SMPC strategy. Detailed experimental procedure is given below.

- **Exp1**. F_2 and F_3 with mechanism-based multi-objective predictive control (MMPC) strategy [46] track L_1. In this case, the dynamic parameters of EVP are uncertain.
- **Exp2**. The surrogate-driven multi-objective predictive control strategy with LQR solver, namely, LMPC [19] is applied to each following vehicle to track L_1.
- **Exp3**. F_2 and F_3 are driven by the SMPC strategy to track L_1.

TABLE III: EXPERIMENTAL PARAMETERS

Symbol	N	L	N_m	T_s	SOC_0	d	N_g
Value	16	9	12	$10Hz$	70%	50m	30

The merits of the proposed strategy involving surrogate-driven modelling and GWO-based multi-objective optimization are listed in TABLE II. Furthermore, TABLE III gives several key experimental parameters.

V. Results and Discussions

In this part, the results of different strategies will be analyzed in terms of three indicators involving safety, comfort and economy for EVP.

A. Driving Safety

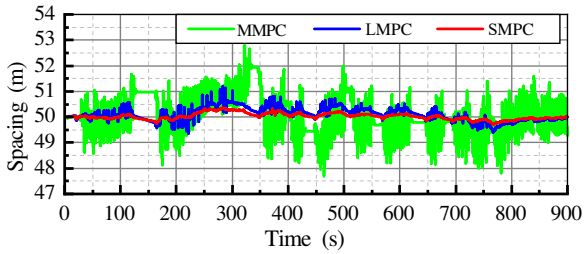

(a) Spacing between L_1 and F_2 with different strategies

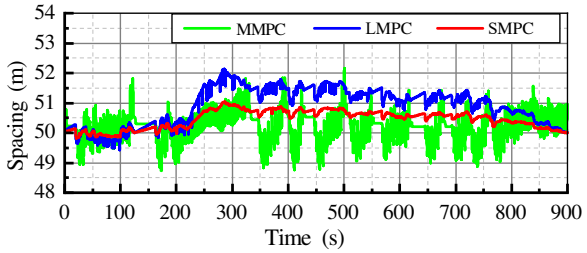

(b) Spacing between F_2 and F_3 with different strategies

Fig. 7. Results of the spacing for EVP

It is clear to see the superiority of our proposed SMPC strategy from Fig. 7. More specifically, F_2 with the MMPC strategy performs an obvious spacing error in Fig. 7(a). The LMPC strategy could maintain consistent spacing within 200s, and then it executes a bigger spacing error at the rest of the time. Comparatively, the proposed SMPC strategy exhibits more stable spacing than the others, which indicates that more robust string stability could be ensured for EVP. Furthermore,

a similar result is also obtained for F_3, see Fig. 7(b) for details. Therefore, these results illustrate that the SMPC strategy outperforms both MMPC and LMPC schemes in terms of driving safety.

B. Driving Comfort

The driving comfort of EVP is investigated by analyzing the velocity and acceleration in Fig. 8. To be more specific, the MMPC strategy exhibits a larger oscillation during velocity tracking, resulting in an uncomfortable driving experience. Apart from situations with rapid velocity fluctuations, the LMPC strategy has the capability to maintain stable tracking of the desired velocity. Note that the SMPC strategy performs the most desirable velocity tracking capability, even amidst intricate velocity scenarios.

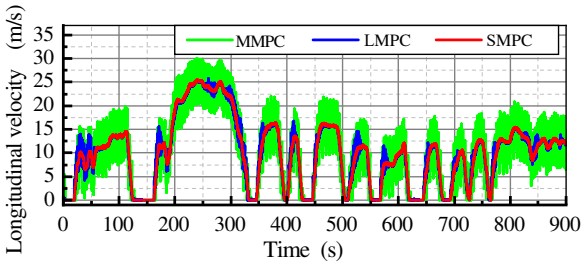

(a) Velocity of F_2 with different strategies

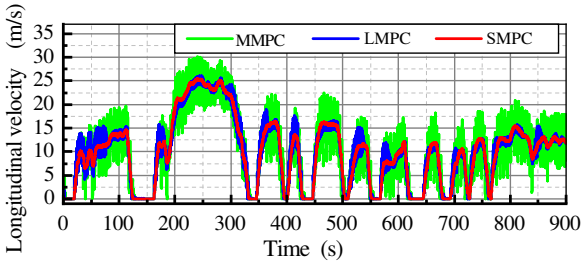

(b) Velocity of F_3 with different strategies

Fig. 8. Results of the velocity for EVP

Furthermore, three evaluation indicators including mode, interquartile range (IQR) and median of acceleration are plotted in Fig. 9. The SMPC strategy exhibits the minimum values compared to others, implying the most stable driving operation. According to the analysis above, the proposed SMPC strategy could provide satisfactory driving experience for drivers than others.

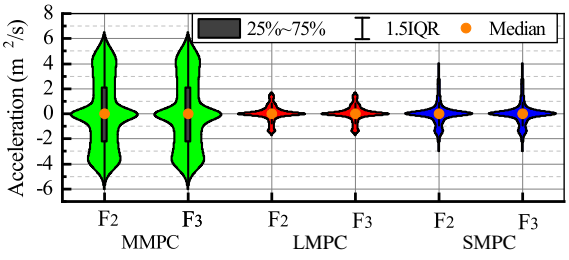

Fig. 9. Results of the acceleration for EVP

C. Driving Economy

The economic objective of EVP aims to enhance battery efficiency, essentially minimizing the decline of SOC. Here, the SOC of each AEV is employed to verify the economy for different strategies. As illustrated in Fig. 10, SOC_0 is set to 70%. With the increase of the accumulated mileage, SOC gradually decreases. The MMPC strategy exhibits a fast decline trend, especially on the high-speed section from 200s to 300s. Upon completing the entire journey, the final SOC of F_2 and F_3 turn to be 57.8% and 58%, respectively. In addition, F_2 and F_3 with the SMPC strategy execute a gradual discharge rate, and the final SOC reaches 61% and 60%. Relatively, the degradation trend of the LMPC strategy is similar to that of the SMPC, but the final SOC changes to 59.2% and 58.7%. It can be seen that the SMPC strategy is superior to the MMPC and LMPC ones in terms of economic efficiency.

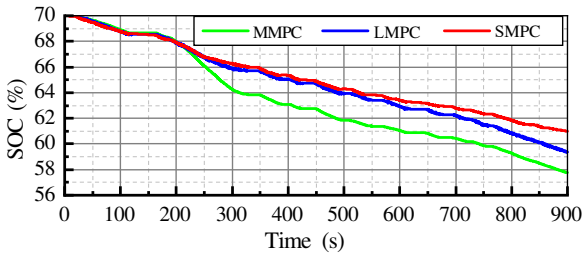

(a) SOC of F_2 with different strategies

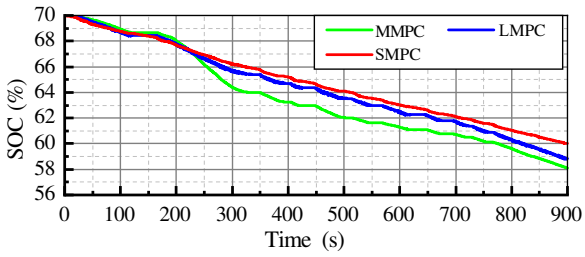

(b) SOC of F_3 with different strategies

Fig. 10. Results of the SOC for EVP

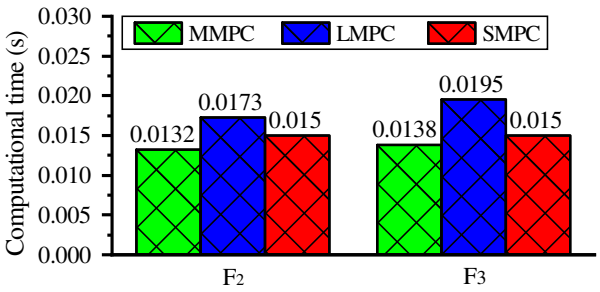

Fig. 11. Computational time of different strategies

D. Computational Efficiency

The computational efficiency of algorithms is also of paramount significance for EVP, affecting real-time platoon

control. Therefore, the average computational time of each sampling interval among three strategies has been presented in Fig. 11. F_2 and F_3 with the MMPC strategy spend the minimal computational time about 0.0132s and 0.0138s, respectively. The LMPC strategy allocates the utmost computational time of 0.0173s and 0.0195s. Meanwhile, the computational time of the SMPC strategy falls within the spectrum between the aforementioned two. This indicates that despite a marginal compromise in computational efficiency, the SMPC strategy can efficiently handle dynamic uncertainty and enhance string stability of EVP.

E. Comprehensive Analysis

To provide a more intricate explanation of the advantages of our proposed SMPC approach, the correlation coefficient method [47] is employed to analyze the aforementioned experiments. The rationale behind this approach is to investigate the correlation between the leading vehicle and the following vehicles. A higher coefficient indicates a greater similarity, signifying a more effective control. Note that the safety index is attributed to velocity and acceleration. As shown in TABLE IV, the proposed SMPC strategy keeps higher coefficients over MMPC and LMPC. Accordingly, the variance values of these results are also demonstrated in Fig. 12. A smaller value indicates a better performance. The proposed SMPC strategy has the minimum coefficient, which implies the optimal comprehensive performance in terms of economy, comfort and safety.

TABLE IV: CORRELATION COEFFICIENT ANALYSIS

Symbol		MMPC	LMPC	SMPC
Safety (S)	F_2	0.8569	0.9293	0.9751
	F_3	0.8424	0.9246	0.9535
Comfort (V, a)	F_2	0.9167	0.9217	0.9845
	F_3	0.9011	0.9341	0.9490
Economy (SOC)	F_2	0.8017	0.8404	0.8773
	F_3	0.8001	0.8446	0.8651

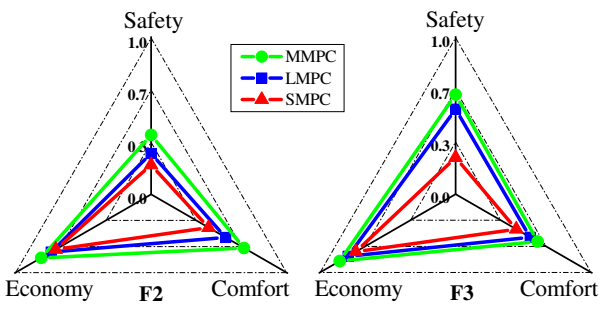

Fig. 12. Variance analysis of different strategies

Additionally, assessing the platoon string stability of the proposed strategy is also essential. The results of spacing among all AEVs keep a reasonable range of approximately 50m within the deviation of 1m. F_2 and F_3 execute a desirable capability in velocity tracking and SOC consumption for EVP. Therefore, it can be concluded that our proposed SMPC strategy could provide a safe, economical and comfortable driving experience for EVP. Furthermore, the proposed strategy could also reduce the calculation burden for EVP.

VI. Conclusion

In this paper, we have developed an SMPC strategy to handle vehicle dynamic uncertainty and multi-objective conflicts for EVP. The subspace identification method has been utilized to establish the surrogate-driven model, so as to alleviate the adverse effects of uncertain dynamics. The optimal predictive sequence is generated by the subspace predictor and utilized to construct a multi-objective cost function. Then, a grey wolf optimizer has been developed to find the optimal solutions among conflicting objectives. Finally, the experimental results have demonstrated that our proposed SMPC strategy enables a more safe, economical and comfortable driving manner for EVP. However, limited experimental scenarios and dataset make it challenging to validate the generalizability of the proposed strategy on complex scenarios. Moreover, several hypotheses are imposed to derive a concise electric vehicle model. This would make it difficult to provide accurate predictions in practical applications. Our future work will be dedicated to broadening the scope of our dataset in several complex driving scenarios. Moreover, exploring the application of our proposed strategy to actual electric vehicles will constitute a distinct research task.

References

[1] U. Z. A. Hamid, *Autonomous, Connected, Electric and Shared Vehicles: Disrupting the Automotive and Mobility Sectors*. SAE International, 2022.

[2] J. Li, Q. Zhou, Y. He, H. Williams, H. Xu, and G. Lu, "Distributed cooperative energy management system of connected hybrid electric vehicles with personalized non-stationary inference," *IEEE Transactions on Transportation Electrification*, vol. 8, no. 2, pp. 2996–3007, 2021.

[3] Y. Wu, Z. Zuo, Y. Wang, Q. Han, and C. Hu, "Distributed data-driven model predictive control for heterogeneous vehicular platoon with uncertain dynamics," *IEEE Transactions on Vehicular Technology*, vol. 72, no. 8, pp. 9969–9983, 2023.

[4] Y. Zheng, S. E. Li, J. Wang, D. Cao, and K. Li, "Stability and scalability of homogeneous vehicular platoon: Study on the influence of information flow topologies," *IEEE Transactions on Intelligent Transportation Systems*, vol. 17, no. 1, pp. 14–26, 2015.

[5] D. Liu, B. Besselink, S. Baldi, W. Yu, and H. L. Trentelman, "An adaptive disturbance decoupling perspective to longitudinal platooning," *IEEE Control Systems Letters*, vol. 6, pp. 668–673, 2022.

[6] D. Liu, B. Besselink, S. Baldi, W. Yu, and H. L. Trentelman, "Output-feedback design of longitudinal platooning with adaptive disturbance decoupling," *IEEE Control Systems Letters*, vol. 6, pp. 3104–3109, 2022.

[7] Y. Liu, C. Zong, C. Dai, H. Zheng, and D. Zhang, "Behavioral decision-making approach for vehicle platoon control: Two noncooperative game models," *IEEE Transactions on Transportation Electrification*, 2023, doi: 10.1109/TTE.2023.3237929.

[8] C. Zhai, Y. Liu, and F. Luo, "A switched control strategy of heterogeneous vehicle platoon for multiple objectives with state constraints," *IEEE Transactions on Intelligent Transportation Systems*, vol. 20, no. 5, pp. 1883–1896, 2018.

[9] Q. Zhou, Y. Zhang, Z. Li, J. Li, H. Xu, and O. Olatunbosun, "Cyber-physical energy-saving control for hybrid aircraft-towing tractor based on online swarm intelligent programming," *IEEE Transactions on Industrial Informatics*, vol. 14, no. 9, pp. 4149–4158, 2017.

[10] S. Vazquez, J. I. Leon, L. G. Franquelo, J. Rodriguez, H. A. Young, A. Marquez, and P. Zanchetta, "Model predictive control: A review of its applications in power electronics," *IEEE Industrial Electronics Magazine*, vol. 8, no. 1, pp. 16–31, 2014.
[11] S. Kouro, M. A. Perez, J. Rodriguez, A. M. Llor, and H. A. Young, "Model predictive control: MPC's role in the evolution of power electronics," *IEEE Industrial Electronics Magazine*, vol. 9, no. 4, pp. 8–21, 2015.
[12] P. Liu, A. Kurt, and U. Ozguner, "Distributed model predictive control for cooperative and flexible vehicle platooning," *IEEE Transactions on Control Systems Technology*, vol. 27, no. 3, pp. 1115–1128, 2018.
[13] S. Feng, Z. Song, Z. Li, Y. Zhang, and L. Li, "Robust platoon control in mixed traffic flow based on tube model predictive control," *IEEE Transactions on Intelligent Vehicles*, vol. 6, no. 4, pp. 711–722, 2021.
[14] L. Jin, M. Čičić, K. H. Johansson, and S. Amin, "Analysis and design of vehicle platooning operations on mixed-traffic highways," *IEEE Transactions on Automatic Control*, vol. 66, no. 10, pp. 4715–4730, 2020.
[15] R. A. Dollar and A. Vahidi, "Efficient and collision-free anticipative cruise control in randomly mixed strings," *IEEE Transactions on Intelligent Vehicles*, vol. 3, no. 4, pp. 439–452, 2018.
[16] J. Bongard, J. Berberich, J. Köhler, and F. Allgöwer, "Robust stability analysis of a simple data-driven model predictive control approach," *IEEE Transactions on Automatic Control*, vol. 68, no. 5, pp. 2625–2637, 2023.
[17] H. Han, Z. Liu, H. Liu, and J. Qiao, "Knowledge-data-driven model predictive control for a class of nonlinear systems," *IEEE Transactions on Systems, Man, and Cybernetics: Systems*, vol. 51, no. 7, pp. 4492–4504, 2019.
[18] Y. Zhang, Y. Huangfu, B. Tan, S. Quan, P. Li, and C. Tian, "A virtual MPC-based artificial neural network controller for pmsm drives in aircraft electric propulsion system," in *2022 IEEE Industry Applications Society Annual Meeting (IAS)*, pp. 1–6, IEEE, 2022.
[19] J. Guo, H. Guo, J. Liu, D. Cao, and H. Chen, "Distributed data-driven predictive control for hybrid connected vehicle platoons with guaranteed robustness and string stability," *IEEE Internet of Things Journal*, vol. 9, no. 17, pp. 16308–16321, 2022.
[20] S. E. Li, R. Li, J. Wang, X. Hu, B. Cheng, and K. Li, "Stabilizing periodic control of automated vehicle platoon with minimized fuel consumption," *IEEE Transactions on Transportation Electrification*, vol. 3, no. 1, pp. 259–271, 2016.
[21] Y. Luo, T. Chen, S. Zhang, and K. Li, "Intelligent hybrid electric vehicle acc with coordinated control of tracking ability, fuel economy, and ride comfort," *IEEE Transactions on Intelligent Transportation Systems*, vol. 16, no. 4, pp. 2303–2308, 2015.
[22] X. T. Yang, K. Huang, Z. Zhang, Z. A. Zhang, and F. Lin, "Eco-driving system for connected automated vehicles: Multi-objective trajectory optimization," *IEEE Transactions on Intelligent Transportation Systems*, vol. 22, no. 12, pp. 7837–7849, 2020.
[23] Y. He, Q. Zhou, M. Makridis, K. Mattas, J. Li, H. Williams, and H. Xu, "Multiobjective co-optimization of cooperative adaptive cruise control and energy management strategy for PHEVs," *IEEE Transactions on Transportation Electrification*, vol. 6, no. 1, pp. 346–355, 2020.
[24] Q. Zhou, W. Zhang, S. Cash, O. Olatunbosun, H. Xu, and G. Lu, "Intelligent sizing of a series hybrid electric power-train system based on chaos-enhanced accelerated particle swarm optimization," *Applied Energy*, vol. 189, pp. 588–601, 2017.
[25] W. Song, Y. Yang, W. Qin, and P. Wheeler, "Switching state selection for model predictive control based on genetic algorithm solution in an indirect matrix converter," *IEEE Transactions on Transportation Electrification*, vol. 8, no. 4, pp. 4496–4508, 2022.
[26] J. Li, X. Deng, Z. Zhan, L. Yu, K. C. Tan, K. Lai, and J. Zhang, "A multipopulation multiobjective ant colony system considering travel and prevention costs for vehicle routing in covid-19-like epidemics," *IEEE Transactions on Intelligent Transportation Systems*, vol. 23, no. 12, pp. 25062–25076, 2022.
[27] X. Sun, Y. Zhang, X. Tian, J. Cao, and J. Zhu, "Speed sensorless control for ipmsms using a modified mras with gray wolf optimization algorithm," *IEEE Transactions on Transportation Electrification*, vol. 8, no. 1, pp. 1326–1337, 2021.
[28] X. Guo, Z. Zhang, L. Qi, S. Liu, Y. Tang, and Z. Zhao, "Stochastic hybrid discrete grey wolf optimizer for multi-objective disassembly sequencing and line balancing planning in disassembling multiple products," *IEEE Transactions on Automation Science and Engineering*, vol. 19, no. 3, pp. 1744–1756, 2021.
[29] J. Li, Q. Zhou, H. Williams, H. Xu, and C. Du, "Cyber-physical data fusion in surrogate-assisted strength pareto evolutionary algorithm for phev energy management optimization," *IEEE Transactions on Industrial Informatics*, vol. 18, no. 6, pp. 4107–4117, 2021.
[30] Y. Zheng, S. E. Li, K. Li, F. Borrelli, and J. K. Hedrick, "Distributed model predictive control for heterogeneous vehicle platoons under unidirectional topologies," *IEEE Transactions on Control Systems Technology*, vol. 25, no. 3, pp. 899–910, 2016.
[31] A. Guha and A. Patra, "State of health estimation of lithium-ion batteries using capacity fade and internal resistance growth models," *IEEE Transactions on Transportation Electrification*, vol. 4, no. 1, pp. 135–146, 2017.
[32] L. Li, W. Cao, H. Yang, and Q. Geng, "Trajectory tracking control for a wheel mobile robot on rough and uneven ground," *Mechatronics*, vol. 83, p. 102741, 2022.
[33] P. Van Overschee and B. De Moor, "A unifying theorem for three subspace system identification algorithms," *Automatica*, vol. 31, no. 12, pp. 1853–1864, 1995.
[34] N. A. Mardi, *Data-driven subspace-based model predictive control*. PhD thesis, Citeseer, 2010.
[35] L. Zhu, F. Tao, Z. Fu, H. Sun, B. Ji, and Q. Chen, "Multiobjective optimization of safety, comfort, fuel economy, and power sources durability for FCHEV in car-following scenarios," *IEEE Transactions on Transportation Electrification*, vol. 9, no. 1, pp. 1797–1808, 2022.
[36] M. Zhu, Y. Wang, Z. Pu, J. Hu, X. Wang, and R. Ke, "Safe, efficient, and comfortable velocity control based on reinforcement learning for autonomous driving," *Transportation Research Part C: Emerging Technologies*, vol. 117, p. 102662, 2020.
[37] J. Luo, D. He, W. Zhu, and H. Du, "Multiobjective platooning of connected and automated vehicles using distributed economic model predictive control," *IEEE Transactions on Intelligent Transportation Systems*, vol. 23, no. 10, pp. 19121–19135, 2022.
[38] X. Hu, X. Zhang, X. Tang, and X. Lin, "Model predictive control of hybrid electric vehicles for fuel economy, emission reductions, and inter-vehicle safety in car-following scenarios," *Energy*, vol. 196, p. 117101, 2020.
[39] S. Mirjalili, S. M. Mirjalili, and A. Lewis, "Grey wolf optimizer," *Advances in Engineering Software*, vol. 69, pp. 46–61, 2014.
[40] V. Bachtiar, E. C. Kerrigan, W. H. Moase, and C. Manzie, "Continuity and monotonicity of the mpc value function with respect to sampling time and prediction horizon," *Automatica*, vol. 63, pp. 330–337, 2016.
[41] H. Lu, Q. Zong, S. Lai, B. Tian, and L. Xie, "Real-time perception-limited motion planning using sampling-based mpc," *IEEE Transactions on Industrial Electronics*, vol. 69, no. 12, pp. 13182–13191, 2022.
[42] S. Xu and H. Peng, "Design, analysis, and experiments of preview path tracking control for autonomous vehicles," *IEEE Transactions on Intelligent Transportation Systems*, vol. 21, no. 1, pp. 48–58, 2019.
[43] H. Gao, B. Cheng, J. Wang, K. Li, J. Zhao, and D. Li, "Object classification using cnn-based fusion of vision and lidar in autonomous vehicle environment," *IEEE Transactions on Industrial Informatics*, vol. 14, no. 9, pp. 4224–4231, 2018.
[44] A. Tuchner and J. Haddad, "Vehicle platoon formation using interpolating control: A laboratory experimental analysis," *Transportation Research Part C: Emerging Technologies*, vol. 84, pp. 21–47, 2017.
[45] C. Bergenhem, S. Shladover, E. Coelingh, C. Englund, and S. Tsugawa, "Overview of platooning systems," in *Proceedings of the 19th ITS World Congress, Oct 22-26, Vienna, Austria (2012)*, 2012.
[46] P. Cortés, M. P. Kazmierkowski, R. M. Kennel, D. E. Quevedo, and J. Rodríguez, "Predictive control in power electronics and drives," *IEEE Transactions on Industrial Electronics*, vol. 55, no. 12, pp. 4312–4324, 2008.
[47] A. G. Asuero, A. Sayago, and A. González, "The correlation coefficient: An overview," *Critical Reviews in Analytical Chemistry*, vol. 36, no. 1, pp. 41–59, 2006.

Yanhong Wu received the M.S. degree in vehicle engineering from Chongqing Jiaotong University, Chongqing, China, in 2020. He is currently pursuing the Ph.D. degree with the School of Electrical Automation and Information Engineering, Tianjin University, Tianjin, China. He is now a visiting student with the University of Birmingham, U.K.

His research interests include surrogate-driven modelling, model predictive control, and their applications on connected and autonomous vehicles.

Zhiqiang Zuo (M'04 - SM'18) received the M.S. degree in control theory and control engineering from Yanshan University, Qinhuangdao, China, in 2001, and the Ph.D. degree in control theory from Peking University, Beijing, China, in 2004.

In 2004, he joined the School of Electrical Automation and Information Engineering, Tianjin University, Tianjin, China, where he is a Full Professor. From 2008 to 2010, he was a Research Fellow with the Department of Mathematics, City University of Hong Kong, Hong Kong. From 2013 to 2014, he was a Visiting Scholar with the University of California at Riverside, Riverside, CA, USA. His current research interests include nonlinear control, robust control, model predictive control, and multiagent systems.

Prof. Zuo is an Associate Editor of the Journal of the Franklin Institute.

Yijing Wang received the M.S. degree in control theory and control engineering from Yanshan University, Qinhuangdao, China, in 2000, and the Ph.D. degree in control theory from Peking University, Beijing, China, in 2004.

In 2004, she joined the School of Electrical Automation and Information Engineering, Tianjin University, Tianjin, China, where she is a Full Professor. Her current research interests include analysis and control of switched/hybrid systems and robust control.

Qiaoni Han received the B.S. and M.S. degrees from the Institute of Electrical Engineering, Yanshan University, China, in 2010 and 2013, respectively, and the Ph.D. degree from the School of Electronic and Electric Engineering, Shanghai Jiao Tong University, Shanghai, China, in 2017. From 2017 to 2019, she was an Assistant Professor with Qingdao University and selected for the Young Talents Program.

She is currently an Associate Professor with the Department of Automation, Tianjin University, Tianjin, China. Her research interests include modelling and optimization of wireless networks, transmission and control of network systems.

Ji Li (Member, IEEE) received the Ph.D. degree in mechanical engineering from the University of Birmingham, U.K., in 2020.

He is currently a Research Fellow and works on the Connected and Autonomous Systems for Electrified Vehicles (CASE-V) at the Birmingham CASE-V Automotive Research and Education Centre. His current research interests include computational intelligence, data-efficient modelling, feature selection, man-machine system, and their applications on connected and AVs.

Quan Zhou (M'17) received his BEng and MEng in vehicle engineering from Wuhan University of Technology, in 2012 and 2015, respectively. He received the Ph.D. in mechanical engineering from the University of Birmingham (UoB) in 2019 that was distinguished by being the school's sole recipient of the UoB Ratcliffe Prize. From 2021 to 2023, she was an Assistant Professor in Automotive Engineering and led the Research Group of Connected and Autonomous Systems for Electrified Vehicles (CASE-V) at UoB.

He is currently a Professor with School of Automotive Studies, Tongji University, Shanghai, China. His research interests include evolutionary computation, reinforcement learning, and their application in vehicular systems.

Hongming Xu received the Ph.D. degree in mechanical engineering from Imperial College London, London, U.K., in 1995.

He is a Professor of energy and automotive engineering at the University of Birmingham, Birmingham, U.K., and the Head of Vehicle and Engine Technology Research Centre. He has six years of industrial experience with Jaguar Land Rover, Coventry, U.K. He has authored and coauthored more than 500 journals and conference publications on advanced vehicle powertrain systems involving both experimental and modelling studies.